Investigation of Solid Solution Hardening in Molybdenum Alloys

I. Wesemann*, A. Hoffmann*, T. Mrotzek**, U. Martin***

* PLANSEE Metall GmbH, Austria

** PLANSEE SE, Austria

*** Technische Universität Bergakademie Freiberg, Germany

Abstract

Mechanical properties of pure molybdenum like yield strength, hardness and creep strength can be modified by alloying elements. The alteration of properties can be described as a result of different mechanisms like solid solution hardening (SSH), particle as well as grain boundary hardening. The aim of this work is to quantify the solid solution hardening effect of different solutes. Therefore the influences of other strength affecting mechanisms like grain boundary hardening or particle hardening have been excluded. Based on the powder metallurgical manufacturing route different molybdenum alloys with Cr, Re, Ta, Ti or W additions were prepared. Vickers hardness measurements at room temperature and tensile tests at 500°C were performed to quantify the hardening effect. Additionally the modulus of rigidity was measured by ultrasonic inspection and the dynamical resonance method. Lattice parameters were measured by means of X-ray diffraction experiments. Applying existing theories of solid solution hardening an attempt was made to separate and quantify dielastic and parelastic effects.

Keywords

Molybdenum alloy, solid solution hardening, chromium, rhenium, tantalum, titanium, tungsten, Hall-Petch hardening, Labusch, Fleischer, Suzuki, modelling, lattice parameter, modulus of rigidity

Introduction

Owing to their outstanding combination of high temperature properties like high melting point, low vapour pressure and high temperature strength molybdenum and its alloys have been in focus for a variety of applications for several decades.

Extensive work on the development of molybdenum based alloys was done in the 1950`s and 1960`s by several authors [1–4]. Most of the work was done with respect to technological properties like hardness, tensile strength, workability and ductile to brittle transition temperature. However, reliable information about solid solution effects are rare. Some authors provide information about parelastic interaction of the different solutes in molybdenum [12]. Comparing the results of different authors the published data regarding hardening rates vs. solute content are widely scattered (Fig. 1), but no values on dielastic interactions are available. Therefore only tendencies regarding the hardening rate of the different alloying elements can be concluded. Furthermore no attempt was made to separate the solid solution

hardening from the other strength influencing effects like particle hardening, grain boundary hardening and texture. Comparable information about sample homogeneity and chemical composition is not available, too.

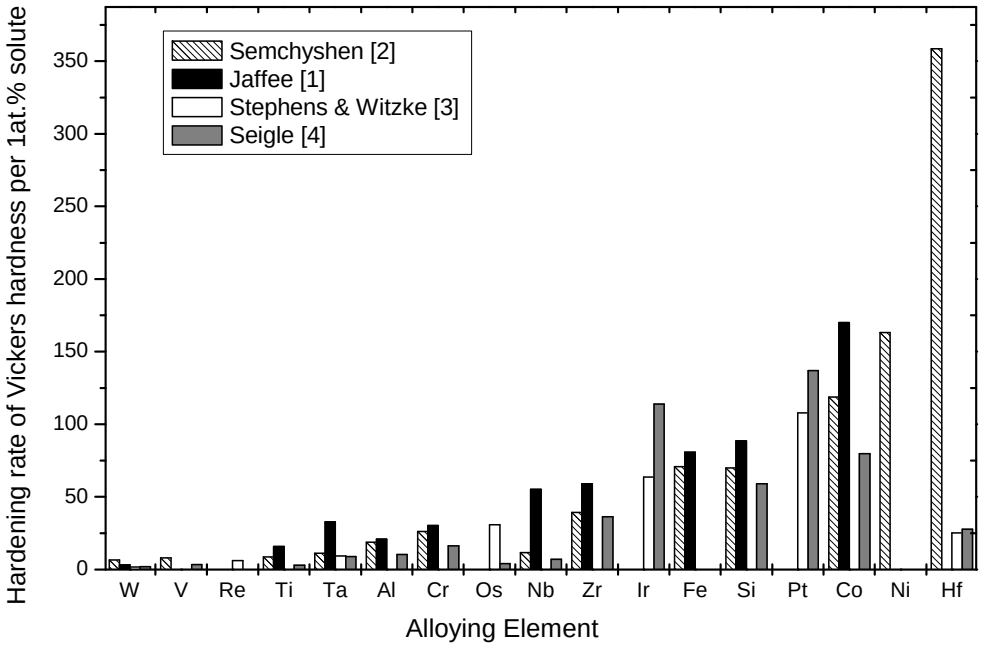

Fig. 1: Vickers hardness increase per atomic % solutes reported by different authors [1] – [4]

An increasing demand for tailored molybdenum alloys requires detailed information about the effectiveness of the individual strength increasing mechanisms in molybdenum. To make precise predictions about SSH in tailored molybdenum alloys it is indispensable to know parelastic and dielastic interactions resulting from the different solutes. Theories from Fleischer, Labusch and Suzuki try to explain these two interactions. Only little information is available which theory is most suitable for describing the SSH in molybdenum alloys.

Therefore one major task of this work was to provide and investigate well defined solid solution alloys. Special attention was paid to the sample homogeneity of the solutes, presence of particles and the level of interstitial impurities. The sample preparation is based on a powder metallurgical manufacturing route. The amount of other non avoidable strength influencing mechanism like grain size and texture has to be quantified and separated.

Another object of the work was the comparison of different models describing SSH in molybdenum. After determination of the increase in strength caused by solid solution hardening as well as the parelastic and dielastic interaction parameters of the different theories were verified with respect to the best match between measured and calculated increase of strength.

Theoretical Considerations

The strength of metals can be modified by work hardening, solute atoms, grain size, particles and the texture. In general a linear superposition of these strength determining mechanisms is assumed for pure metals.

SSH results from interactions between solute atoms and dislocations. These interactions can be classified in parelastic interactions, dielastic interactions, interactions resulting from atomic ordering, chemical effects and interactions resulting in changes of the local electronic structure [5-6]. The parelastic interaction is a result of the interaction between the dilatation of the lattice near the solute atom and the dilatation around the stress field of a dislocation. The parelastic interaction δ is best described by the change of the lattice constant with solute alloying content *c* [7]:

$$\delta = \frac{1}{a} \cdot \frac{da}{dc} \tag{1}$$

According to R. L. Fleischer [7] the dielastic interaction is a result of local changes of bonding energies between the solute atom and the matrix. They are best quantified by the change of the modulus of rigidity *G* with alloying content *c* [6].

$$\eta' = \frac{\eta}{1 + \frac{1}{2}|\eta|}, \text{ with } \eta = \frac{1}{G} \cdot \frac{dG}{dc} \tag{2)(3}$$

Interactions like atom ordering, chemical effects or changes of the local electron structure are very difficult to measure and not to quantify as easy as the parelastic solid solution hardening effect. A useful review about these interactions can be found in [6].

For the modelling of SSH the theories of Fleischer, Labusch and Suzuki have been established [9]. These theories can be summarized by one simple formula (4). The contribution of solid solution hardening τ_c to the total critical shear strength depends on the concentration *c,* the exponent *p,* a hardening parameter ***ε*** and the exponent *q* in case of Fleischer and Labusch [6]. The parameter ***ε*** is a combination of δ and η' and a parameter α which assess δ and η'. Suzuki defines an interaction energy E_W instead of ε which also incorporates parelastic and dielastic interactions. It should be noted that a different parameter η'' is defined. This parameter considers a non linear superpositioning of parelastic and dielastic interactions and requires an additional material constant based on measurements for iron [8]. In addition the modulus of rigidity at room temperature G_0 and the modulus of rigidity *G(T)* at certain temperature *T* have to be determined for the calculation of E_W. A special feature of the theory by Suzuki is the consideration of the temperature dependency. For simplification H. Hattendorf und R. Büchner have simplified the complex system of non linear equations by Suzuki [10].

$$\tau_c \sim \text{const} \cdot G(T) \cdot \varepsilon^p \cdot c^q \qquad [13] \tag{4}$$

Table I: Overview of parameters and boundary conditions for the different theories describing SSH

Parameter:	**Fleischer:**	**Labusch:**	**Suzuki:**
ε, E_w	$\varepsilon_F = \lvert\eta' + \alpha\delta\rvert$*	$\varepsilon_L = \sqrt{\eta'^2 + \alpha^2\delta^2}$	$E_W = 0.122eV(1.52\delta + \eta'') \cdot \frac{G(T)}{G_0}$

p, q, Z	p = 3/2;
	q = 1/2;
	Z_F = 760
		p = 4/3;
		q = 2/3;
		Z_L = 550
			p = 2;
			q = 1

τ_c	$\tau_{cF} = \frac{1}{Z_F} G\varepsilon_F^{\frac{3}{2}} c^{\frac{1}{2}}$	$\tau_{cL} = \frac{1}{Z_L} G\varepsilon_L^{\frac{4}{3}} c^{\frac{2}{3}}$	$\tau_{cS} = \frac{E_w^2 \cdot c}{kTb^3}$ b… Burgers vector
Boundary conditions	T = 0K; c < 0.1%	T = 0K; c > 0.1% possible	T > 0K possible c > 0.1% possible valid for b.c.c. iron
Reference	[6, 8]	[8]	[8, 10]

* for screw dislocations [14]

Sample Preparation

Alloying elements were selected with respect to the solubility limits in the molybdenum matrix, the availability and the limits were implied by the powder metallurgical manufacturing route. Other important factors are chemical stability of the alloying elements during the sintering process in a hydrogen atmosphere, density after sintering and sufficient deformability after sintering in order to produce samples with a relative density >99.5%.

According to these requirements molybdenum alloys with 0.5-3.0% chromium, 0.5 -5.0% rhenium, 0.5-3.0% tantalum, 0.5-4.0% titanium and 1.0-18.3% tungsten were produced by the manufacturing route as listed in Fig. 2. All compositions are given on atomic percent.

Molybdenum powder (Fischer Sub Sieve Size FSSS=4.7µm) was blended together with commercial available powders of chromium (FSSS<36µm) and tantalum (FSSS<32µm). Molybdenum-rhenium as well as molybdenum- tungsten alloys were produced by blending powders of the standard alloys Mo41wt.%Re (FSSS=4.5µm) and Mo30wt.%W (FSSS=4µm) with molybdenum powder. Titanium was added by Titaniumhydride. Samples with a diameter of 78 mm and a sample height of 110 mm were pressed by cold isostatic pressing. Sintering temperatures as well as the temperature and time for solution annealing have to be selected with respect to the homogeneity of the alloying elements and the risk of evaporation during the high temperature annealing process (Fig. 2). Forging was done in axial direction of the cylinders with a total degree of deformation of φ_{total} = 1.5. Forging increments φ_{ind}, forging temperature and the temperature for the intermediate annealing were selected with respect to the expected high temperature strength. The solution annealing was done as very last process step to get rid of work hardening. As reference a pure molybdenum sample was prepared with an identical manufacturing route as for the molybdenum-titanium alloys.

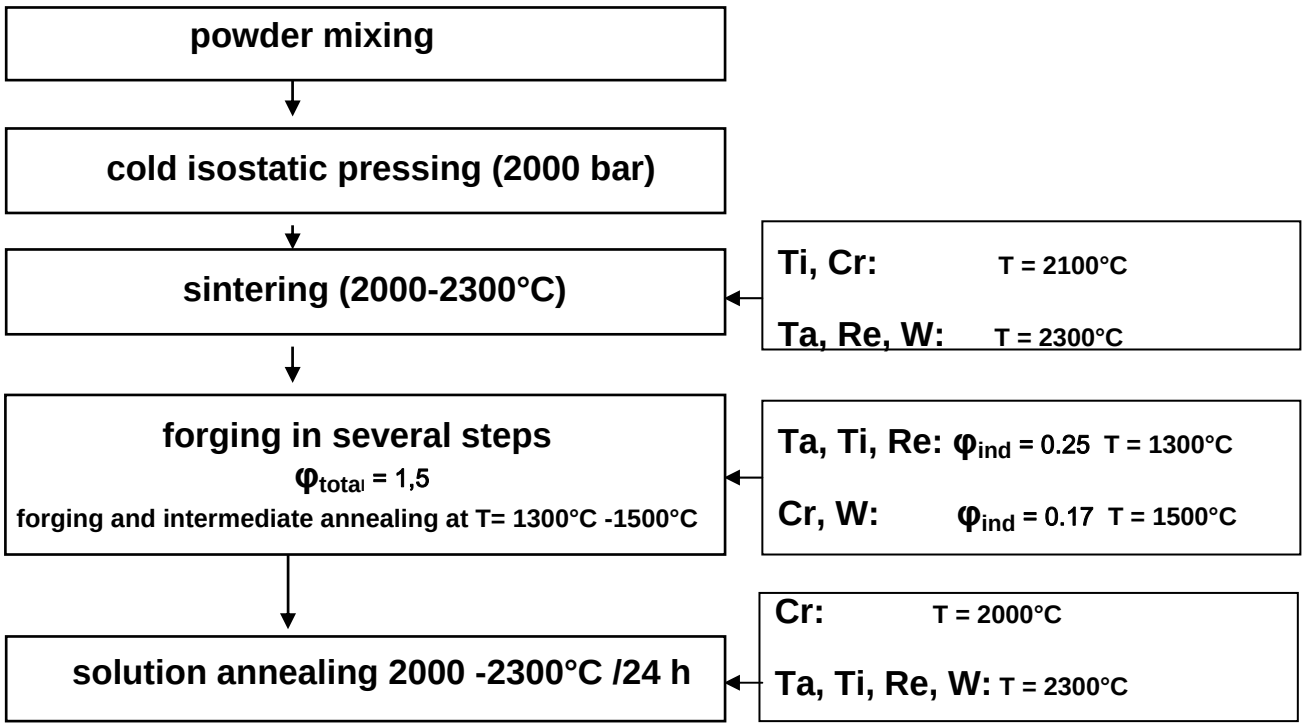

Fig. 2: Powder metallurgical manufacturing route for the preparation of the molybdenum alloys

Characterisation

After the 24h final heat treatment the density, chemical composition, homogeneity of the solute, grain size and texture of the samples were investigated. The mean grain size was determined following ASTM E112-96. The total amount of alloying elements was determined by means of Inductively Coupled Plasma Optical Atom Emission Spectrometry (ICP-OES) for chromium, tantalum, titanium and tungsten and X-Ray Fluorescent Analysis (XFA) for rhenium. The interstitial elements oxygen, nitrogen and hydrogen were determined by Carrier Gas Hot Extraction (CE). Combustion Analyses (CA) was used for carbon. The distribution of the alloying elements after the solution annealing was characterised by Electron Probe Micro Analyser (EPMA) line scans with a step size of 10 µm on a total length of 3000 µm at the TUBA Freiberg on a JOEL JXA 8900RL. Taylor factors were determined from Electron Back Scatter Diffraction (EBSD) measurements of selected samples. The equipment was a LEO Gemini 1530 FEG in combination with a HKL NORDLYS detector system. The analyzed area was 4 mm x 2.4 mm in transversal direction of the tensile specimen.

Mechanical characterization at room temperature was done by Vickers hardness HV10 measurement. Tensile tests could not be performed at room temperature because of elastic fracture of the alloys. At 500°C tensile tests with a strain rate of $\dot{\varepsilon} = 2.0 \cdot 10^{-3} s^{-1}$ were performed with a ZWICK-MAYTEC RMC 100 testing device.

In order to determine the parelastic interaction lattice parameters were determined. The measurement was done in θ / 2θ mode with a step width of 0.02° using a CuK_α radiation at 40kV / 30mA. For monochromatisation a carbon monochromator was used. The large grain size after final solution annealing caused a pseudo texture effect by a low number of reflexes. Therefore the sample position was shifted in order to have at least 4 reflexes.

The effect of dielastic interaction was characterised by the measurement of change in modulus of rigidity. The modulus of rigidity *G* can be determined by velocity of transversal ultrasonic waves c_T in a metal with known density ρ. Transversal ultransonic waves show a low transmittance. Therefore an attempt was made to dertermine *G* without direct measurement of c_T at room temperature. Such a method is described by M. B. Reynolds [11]. Sample diameter *d* and the time Δt between the 1st and 2nd back wall echo and the velocity of longitudinal ultrasonic waves c_L have to be determined. For the verification of the ultra sonic measurements additional measurements were carried out with the ELASTOMAT. The ELASTOMAT excites the sample with different ultra sonic frequencies and the resonance frequencies are determined. Thereby the modulus of elasticity *E* and the Poisson ratio ν can be determined and the modulus of rigidity can be calculated. This comparitive measurement was done for molybdenum-titanium and molybdenum-tungsten alloys.

The effect of grain size hardening was determined with a pure molybdenum reference sample as well as on PLANSEE standard molybdenum rods with a total degree of deformation of φ_{total} = 3.4. The grain size on the molybdenum rods was altered by variation of the annealing temperature between 1300°C and 2300°C. Annealing time was constant for 1 hour. These samples were tested by Vickers hardness HV10 at room temperature and compression tests at 500°C with a deformation rate of $\dot{\varepsilon} = 2.0 \cdot 10^{-3} s^{-1}$.

Results

Except for the molybdenum-titanium alloys chemical analysis revealed interstitial impurities below 1 ppm for hydrogen and below 5 ppm for nitrogen, and carbon. The molybdenum-titanium alloys with titanium content above 2% showed oxygen content of 150-350 ppm. SEM analysis in combination with EDX revealed oxygen containing titanium particles (presumably titanium oxide) for these alloys even after applying a 2300°C annealing.

Even at 2300°C a complete homogeneous distribution of the alloying elements could not be achieved for the molybdenum- tungsten and molybdenum-rhenium alloys, although the whole alloying content was in solid solution (EPMA measurements in fig. 5 and fig. 6). Particles were observed for molybdenum-tantalum and molybdenum-titanium alloys with high alloying content after a 2000°C annealing. After an additional 2300°C annealing the molybdenum- tantalum alloys were completely homogenised (EPMA measurements in Fig. 3 and Fig. 4) while very few particles remained present in the high content molybdenum-titanium alloys.

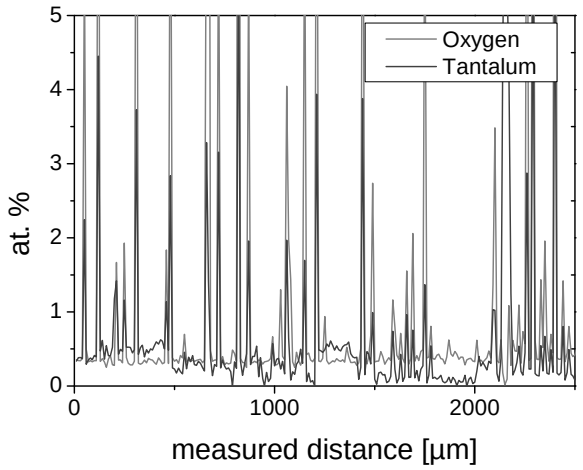

Fig. 3: Tantalum and oxygen distribution in molybdneum 1%-tantalum alloy after 2000°C annealing for 24 h

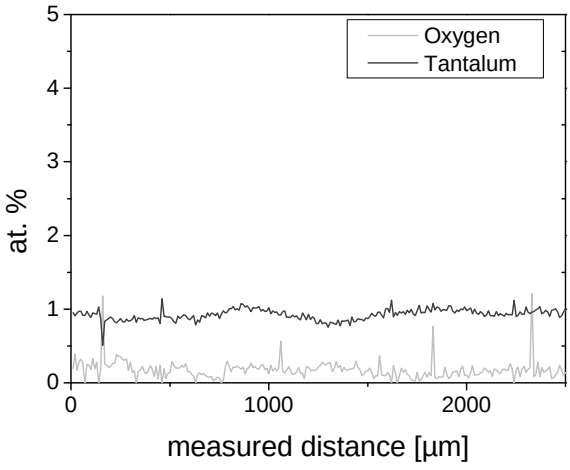

Fig. 4: Tantalum and oxygen distribution in molybdneum 1%-tantalum alloy after 2300°C annealing for 24 h

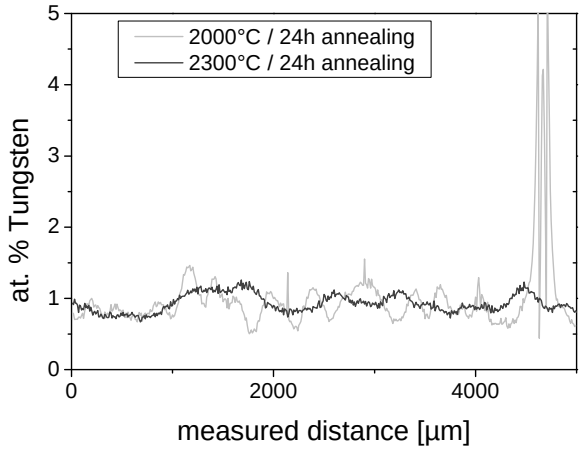

Fig. 5: Tungsten distribution for molybdenum 1% tungsten alloy after 2000°C and 2300°C annealing

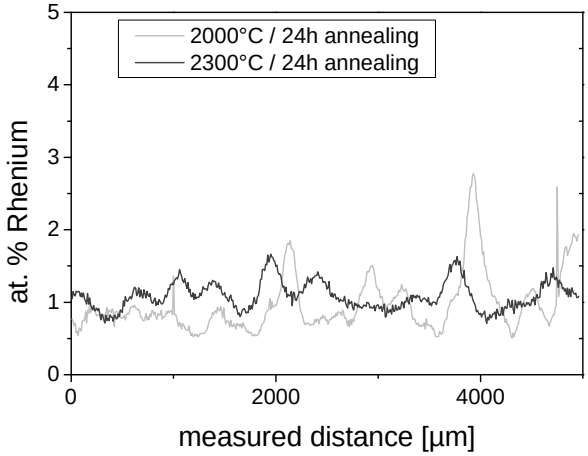

Fig. 6: Rhenium distribution for molybdenum 1% rhenium alloy after 2000°C and 2300°C annealing

The relative density was above 99.5% for all samples except the molybdenum-tantalum with a density above 98.5%. The lower density for molybdenum-tantalum alloys can be explained by the formation of oxygen containing tantalum particles during the sintering. All alloys showed smaller grain sizes with increasing alloying content except the molybdenum-tantalum alloys. Texture measurements revealed a weak texture with Taylor factors of 2.87-3.05. This is close to the theoretical value of texture free b.c.c. metals.

The moduli of rigidity determined by ultra sonic inspection are shown in table II – table VI. The calculated dG/dc values are shown in Table VII. These values are in a good agreement with the values determined by the ELASTOMAT. For the molybdenum-tantalum alloys the measurement of the modulus of rigidity by ultrasonic inspection failed. Therefore values calculated by Vegards law were used.

Lattice parameters showed deviation from the Vegard´s rule for titanium, rhenium but were in good agreement with measured lattice parameters reported in literature [12].

The tensile properties at 500°C are shown in table II- table VI. An upper and lower yield point was observed for some alloys. At 500°C molybdenum-chromium alloys show the highest hardening rate,

followed by tantalum. Rhenium exhibits a moderate hardening rate while SSH was only very weak for titanium and tungsten at this temperature. The hardness values at room temperature showed a continuous increase with increasing solute content for molybdenum-tantalum, molybdenum-titanium and molybdenum-tungsten alloys (Fig. 7). For the molybdenum-chromium alloys a decrease in the Vickers hardness for very low solute content (0.5%Cr) was observed. At higher concentrations SSH was observed. Rhenium showed a similar phenomenon of a decreasing Vickers hardness up to concentrations of 3% rhenium. This effect is known as solid solution softening effect in literature and can not be described by SSH theories. For the hardening rate dHV10/dc of rhenium a literature value was used [3]. In [3] the alloy softening effect has a weak impact on the total hardening rate for alloy containing up to 41 wt.% rhenium.

Table II: Material parameters determined on the molybdenum-chromium alloys and pure molybdenum

	Mo	**Mo0.5Cr**	**Mo1.0Cr**	**Mo2.0Cr**	**Mo3.0Cr**
Measured solute [at.%]	-	0.6	1.0	2.0	3.0
Grain size [µm]	367	374	284	189	177
Taylor factor	2.91	n.d.	2.99	n.d.	3.05
Lattice parameter [Å]	3.14779	3.14763	3.14809	3.14564	3.14522
Modulus of rigidity [GPa]	n.d.	117.5	117.4	116.0	115.7
$R_{p0.2}$ / R_{eH} at 500°C [MPa]	28 / -	n.d.	81 / -	143 / -	- / 206
R_m at 500°C [MPa]	252	n.d.	324	424	353
A at 500°C [%]	52	n.d.	38.1	20.9	5.7

Table III: Material parameters determined on the molybdenum-rhenium alloys

	Mo0.5Re	**Mo1.0Re**	**Mo2.0Re**	**Mo3.0Re**	**Mo5.0Re**
Measured solute [at.%]	0.5	1.0	2.0	3.0	5.0
Grain size [µm]	245	248	254	225	170
Taylor factor	n.d.	n.d.	2.88	n.d.	2.89
Lattice parameter [Å]	3.14763	3.14809	3.14674	3.14564	3.14522
Modulus of rigidity [GPa]	119.2	119.8	122.1	123	122.6
$R_{p0.2}$ / R_{eH} at 500°C [MPa]	n.d.	n.d.	- / 58	- / 95	- / 136
R_m at 500°C [MPa]	n.d.	n.d.	313	352	385
A at 500°C [%]	n.d.	n.d.	53.9	47.7	40

Table IV: Material parameters determined on the molybdenum-tantalum alloys

	Mo0.5Ta	**Mo1.0Ta**	**Mo2.0Ta**	**Mo3.0Ta**
Measured solute [at.%]	0.4	0.9	2.0	3.0
Grain size [µm]	173	220	223	266
Taylor factor	n.d.	n.d.	n.d.	2.93
Lattice parameter [Å]	3.1491	3.14966	3.1499	3.152
Modulus of rigidity [GPa]	n.d.	n.d.	n.d.	n.d.
$R_{p0.2}$ / R_{eH} at 500°C [MPa]	n.d.	- / 58	- / 106	- / 122
R_m at 500°C [MPa]	n.d.	304	372	384
A at 500°C [%]	n.d.	45.9	41.8	39.5

Table V: Material parameters determined on the molybdenum-titanium alloys

	Mo1.0Ti	**Mo2.0Ti**	**Mo3.0Ti**	**Mo4.0Ti**
Measured solute [at.%]	1.0	2.0	3.1	4.0
Grain size [µm]	270	258	206	186
Taylor factor	n.d.	2.96	n.d.	2.87
Lattice parameter [Å]	3.14883	3.14806	3.14831	3.14814
Modulus of rigidity [GPa]	118.2	118.0	116.2	115.2
$R_{p0.2}$ / R_{eH} at 500°C [MPa]	n.d.	46 / -	41 / -	48 / -
R_m at 500°C [MPa]	n.d.	256	311	277
A at 500°C [%]	n.d.	32.1	43.2	29

Table VI: Material parameters determined on the molybdenum-tungsten alloys

	Mo1.0W	**Mo2.7W**	**Mo5.5W**	**Mo11.5W**	**Mo18.3W**
Measured solute [at.%]	1.0	2.8	5.5	11.3	18.4
Grain size [µm]	558	408	250	133	84
Taylor factor	n.d.	n.d.	2.89	n.d.	2.93
Lattice parameter [Å]	3.14798	n.d.	3.14918	3.15066	3.15425
Modulus of rigidity [GPa]	n.d.	116.3	118.3	120.9	122.5
$R_{p0.2}$ / R_{eH} at 500°C [MPa]	n.d.	n.d.	- / 57	- / 102	- / 116
R_m at 500°C [MPa]	n.d.	n.d.	301	365	394
A at 500°C [%]	n.d.	n.d.	45	46.8	45.1

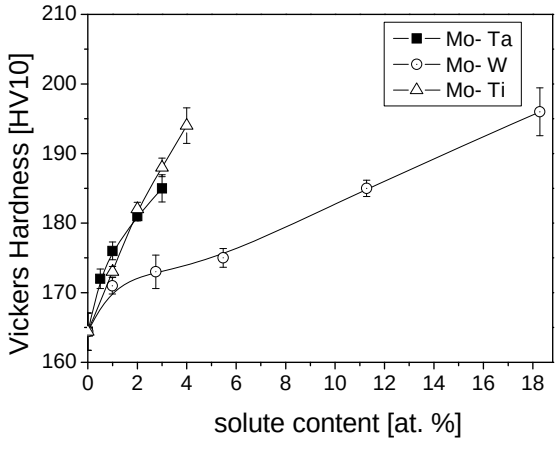

Fig. 7: Vickers hardness measurement depending on the solute content for tantalum, titanium and tungsten

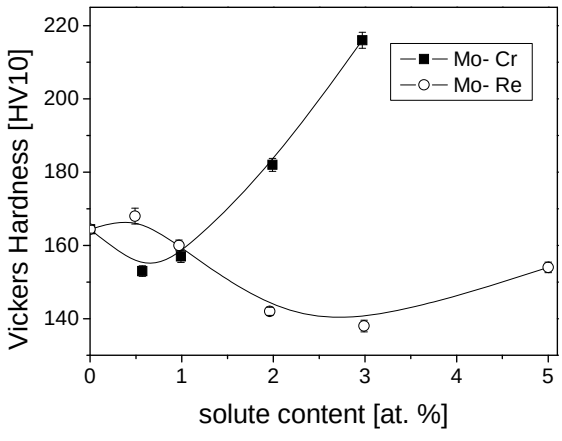

Fig. 8: Vickers hardness measurement depending on the solute content for chromium and rhenium

Fig. 9 shows the plot of the inverse grain size versus $R_{d0.2}$ at 500°C for pure molybdenum. The linear fit procedure revealed the following relations for $R_{d0.2}$ at 500°C and HV10 at room temperature:

$$R_{d\,0.2} = 9.7(\pm 11.4)MPa + 0.595(\pm 0.085) \cdot \frac{1}{\sqrt{d}} MPa \quad (7)$$

$$HV10 = 159.8(\pm 2.6)HV10 + 0.102(\pm 0.018) \cdot \frac{1}{\sqrt{d}} HV10 \quad (8)$$

A week Hall-Petch hardening is observed for molybdenum at room temperature. At 500°C Hall-Petch hardening in pure molybdenum was strong for grain sizes below 50µm. The lattice friction is almost negligible with 9.7MPa at 500°C. This is due to the thermal activation at 500°C. The investigated solid solution alloys showed grains sizes larger than 80µm, therefore the impact on the yield strength was quite low for these alloys. Nevertheless the measured hardness values and $R_{p0.2}$ values were corrected. For simplification a linear superposition of the different hardening mechanisms was assumed. The use of the Hall-Petch relation of pure molybdenum for molybdenum alloys is a further simplification. The effect of texture was corrected by multiplying the measured yield strength by the ratio of the theoretical Taylor factor for randomly orientated molybdenum and the actually measured Taylor factor. The corresponding corrected values for the solid solution hardening are shown in Table VII.

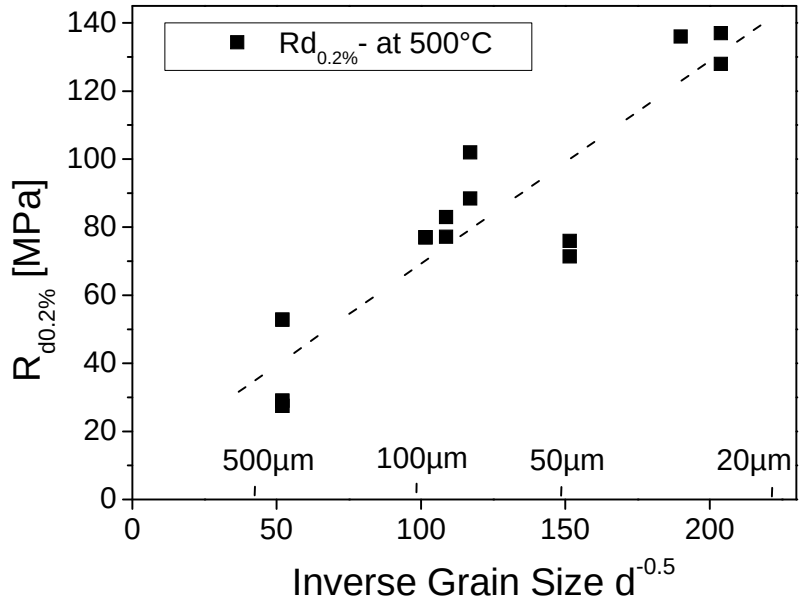

Fig. 9: Hall- Petch- Plot for pure molybdenum at 500°C

Table VII: Determined changes in lattice parameter and modulus of rigidity (calculated for tantalum); hardening rate for the different alloying elements at room temperature and 500°C

	Cr	Re	Ta	Ti	W
da / dc (RT) [nm]	-0,02831	-0,00644	-0,01184	0.00044	0,00340
dG / dc Ultrasonic [GPa]	-81.8	78.6	*-57(calc.)*	-106.7	38.4
dG / dc ELASTOMAT [GPa]	-	-	-	-132.5	32.2
$(dHV10\ /dc)_{corr}$ (RT) [HV10]	2519	614	612	690	118
$(dR_{p0.2}/dc)_{corr}$ (500°C) [MPa]	5248	1795	2887	144	307

The applicability of the different solid solution theories was tested by comparing the correlation between the actually measured hardening rate with the calculated hardening rate. For the calculation of the theoretical hardening rate the parameters δ (eq. 1) and η' (eq. 2) were calculated by the measured changes in lattice parameter and modulus of rigidity. The value α (table I) was determined by a fitting procedure looking for the best match between the experimentally determined ε as well as measured and calculated hardening rates. This procedure was done for the theory of Fleischer and Labusch. At room temperature the best agreement was found for the hardening parameter of Labusch with a $\alpha = 18$ (R^2=0.98) in Fig. 10. Fleischers theory showed good correlation for $\alpha = 9$ (R^2=0.92). For the theory of Suzuki the parameter E_W was calculated according to [10].

Comparing the calculated solid solution hardening with the measured the best agreement was found for Labusch (Fig. 12). Although the SSH theory of Fleischer was developed for concentrations below 1% solute the calculated values show a good agreement with the measured hardening rate at room temperature.

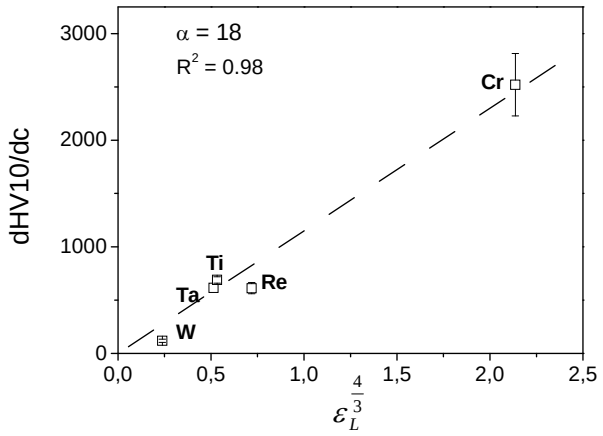

Fig. 10: Correlation between hardening parameter for Labusch and the measured soild solution hardening at room temperature with the best fit for $\alpha = 18$

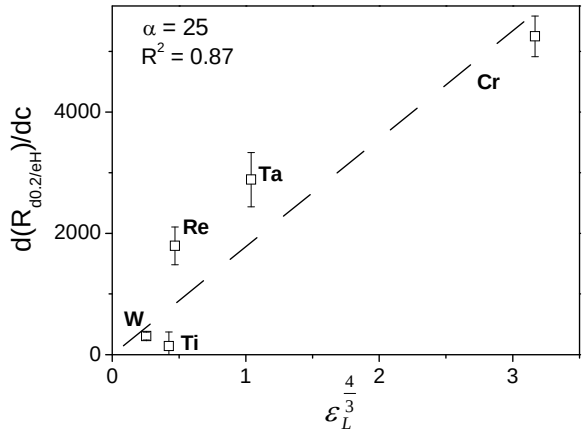

Fig. 11: Correlation between hardening parameter for Labusch and the measured soild solution hardening at 500°C with the best fit for α = 25

The same procedure was carried out for solid solution hardening at 500°C in Fig. 11. Dielastic interactions at 500°C were calculated from the modulus of rigidity of the pure metals at 500°C and assuming Vegard`s law for the alloys. For the parelastic interaction at 500°C the room temperature values were used because no data were available at 500°C. The calculation according to Labusch revealed good agreement for $\alpha = 25$, R^2=0.87. The increase in α from 18 to 25 implies a higher impact of the parelastic interactions. This gives evidence that the influence of dislocations with edge character on the deformation has increased at 500°C. For the theory of Fleischer the best correlation was found to be unrealistically high with a value of α >100, R^2=0.59. The quality of the fit became worse for both theories compared to room temperature. This is probably due to the increasing degree of thermal activation of dislocation movement at 500°C which is not considered in both theories. Nevertheless the theory of Labusch showed still some accordance. The high solute content in the investigated alloys may result in non- discrete obstacles which can not be overcome easily by thermal activation. Labusch´s theory considers these high concentrations with c > 1% in his theory. This may explain the remaining agreement at a temperature of 500°C.

Although Suzuki considers thermal activation the results were even worse. The correlation between calculated and experimentally determined values show a low degree of correlation with R^2=0.16. The bad results are attributed to the definition of E_W and δ" (table I). These two parameters were defined and proofed for iron but not for molybdenum.

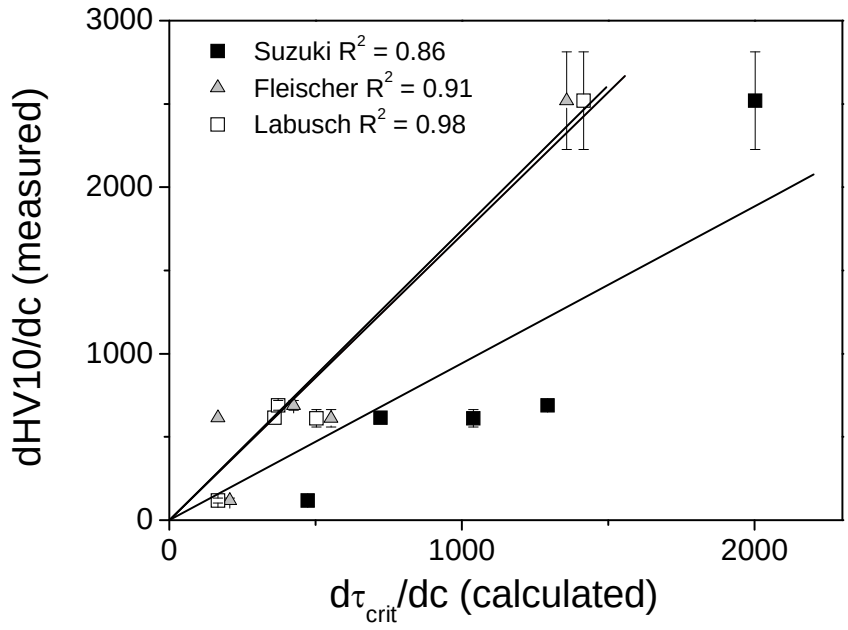

Fig. 12: Comparison of the calculated solid solution hardening dτcrit/dc by the different theories and the actually measured solid solution hardening dHV10/dc at room temperature

Conclusions

The sample characterisation has shown that the manufacturing of homogeneous molybdenum solid solution alloys by powder metallurgy is quite difficult. For a complete homogenization long lasting high temperature solution annealing is required which resulted in significant grain growth. Large grain complicated the determination of the lattice parameters and modulus of rigidity.

Except for the molybdenum-tantalum alloys all other alloys undergo a continuous decrease in grain size with increasing alloy content. At room temperature the molybdenum-chromium alloys and molybdenum-rhenium alloys showed solid solution softening at concentrations up to 1% and 3% respectively. At higher concentrations solid solution hardening was observed. Chromium as alloying element exhibited the highest hardening rate at room temperature followed by titanium, tantalum and rhenium. Tungsten shows a weak solid solution hardening. At 500°C molybdenum-chromium showed the highest solid solution hardening. Moderate hardening was observed for molybdenum-tantalum and molybdenum-rhenium while molybdenum-tungsten and molybdenum-titanium showed only very low solid solution hardening at this temperature. A strong grain size hardening effect was observed for pure molybdenum at 500°C for grain sizes below 50µm. The grain size effect was negligible for the investigated alloys which showed grain sizes above 80µm.

To describe the solid solution hardening in molybdenum the theory of Labsuch is most suitable at room temperature. Although the theory of Labusch was developed for solid solution hardening at 0K, it is still in good agreement at 500°C. Fleischer´s theory showed good agreement at room temperature, too, but

can not be applied at 500°C. Both theories yield high values for α which indicates that dislocations with edge character have significant influence on the SSH in molybdenum. With increasing deformation temperature the impact of dislocations with edge character further increases. The SSH theory of Suzuki has to be further developed for molybdenum. Material parameters for the calculation of E_W have to be estimated for molybdenum instead of using the parameters of iron in the future.

Acknowledgement

The authors would like to thank the University of Erlangen-Nürnberg, Lehrstuhl I (Allgemeine Werkstoffeigenschaften) for the experimental determination of the modulus of rigidity by means of the ELASTOMAT. The authors also acknowledge the support of Dr. rer. nat. D. Heger and Dipl.-Phys. G. Schreiber in experimental work.

References

1. J. J. Harwood, *The Metal Molybdenum – Proceeding*, R.I. Jaffee, American Society for Metals, Ohio, 331-364, (1958)

2. J. J Harwood, *The Metal Molybdenum – Proceeding*, M. Semchyshen, American Society for Metals, Ohio, 281-329, (1958)

3. J. R. Stephens, W. R. Witzke, *Journal of Less- Common Metals* 29, 325-342 (1972)

4. N. E. Promisel, *The Science and Technology of Tungsten, Tantalum, Molybdenum, Niobium and their Alloys – Conference on Refractory Metals held at Oslo Univeristy Centre*, L. L. Seigle, Pergamon Press, Oxford S. 63–93 (1964)

5. J. Friedel, *Dislocations*, 351-366, Pergamon Press, Paris, (1964)

6. P. Haasen, *Zeitschrift für Metallkunde* Bd. 55, 55-60, (1964)

7. R. L. Fleischer, Acta Metallurgica Vol. 9, 203-209, (1963)

8. L. A. Gypen, A. Deruyttere, Scripta Metallurgica Vol. 15, 815- 820, (1981)

9. R. Labusch, Phys. Stat. Sol., Vol. 41, 659-669, (1970)

10. H. Hattendorf, A. R. Büchner, Zeitschrift für Metallkunde Bd 83, 690–698, (1992)

11. M. B. Reynolds, Trans. Am. Soc. For Metals Vol. 45, 839-861, (1953)

12. W. B. Pearson, *Structures of Metals and Alloys*, Pergamon Press, London, (1958)

13. P. Jax, P. Kratochvil, P. Haasen, Acta. Metallugica Vol. 18, 237-245, (1970)

14. B.L. Mordike, Phys. Stat. Sol. (a), 35, 303-308, (1976)